environmental microbiology

Environmental Microbiology (2018) **00**(00), 00–00 doi:10.1111/1462-2920.14054

A novel MADS-box transcription factor *PstMCM1-1* is responsible for full virulence of *Puccinia striiformis* f. sp. *tritici*

Xiaoguo Zhu,[1] Min Jiao,[1] Jia Guo,[1] Peng Liu,[1] Chenglong Tan,[1] Qian Yang,[1] Yang Zhang,[1] Ralf Thomas Voegele,[2] Zhensheng Kang[1]* and Jun Guo[1]*

[1]*State Key Laboratory of Crop Stress Biology for Arid Areas, College of Plant Protection, Northwest A&F University, Yangling, Shaanxi, 712100, China.*
[2]*Department of Phytopathology, Institute of Phytomedicine, Faculty of Agricultural Sciences, University of Hohenheim, Stuttgart, 70599, Germany.*

Summary

In many eukaryotes, transcription factor MCM1 gene plays crucial roles in regulating mating processes and pathogenesis by interacting with other co-factors. However, little is known about the role of MCM1 in rust fungi. Here, we identified two MCM1 orthologs, *PstMCM1-1* and *PstMCM1-2*, in the stripe rust pathogen *Puccinia striiformis* f. sp. *tritici* (*Pst*). Sequence analysis indicated that both *PstMCM1-1* and *PstMCM1-2* contain conserved MADS domains and that *PstMCM1-1* belongs to a group of SRF-like proteins that are evolutionarily specific to rust fungi. Yeast two-hybrid assays indicated that PstMCM1-1 interacts with transcription factors PstSTE12 and PstbE1. *PstMCM1-1* was found to be highly induced during early infection stages in wheat and during pycniospore formation on the alternate host barberry (*Berberis shensiana*). *PstMCM1-1* could complement the lethal phenotype and mating defects in a *mcm1* mutant of *Saccharomyces cerevisiae*. In addition, it partially complemented the defects in appressorium formation and plant infection in a *Magnaporthe oryzae Momcm1* mutant. Knock down of *PstMCM1-1* resulted in a significant reduction of hyphal extension and haustorium formation and the virulence of *Pst* on wheat. Our results suggest that *PstMCM1-1* plays important roles in the regulation of mating and pathogenesis of *Pst* most likely by interacting with co-factors.

Received 7 September, 2017; revised 27 December, 2017; accepted 21 January, 2018. For correspondence. *E-mail: guojunwgq@nwsuaf.edu.cn; Tel./Fax +862987082439. E-mail: kangzs@nwsuaf.edu.cn; Tel./Fax +862987080061.

Introduction

The MADS-box family is a type of conserved transcription factors that widely exist in eukaryotic organisms, including fungi, plants, insects, amphibians and mammals (Shore and Sharrocks, 1995; Zhou *et al*., 2011). All these proteins contain a conserved DNA-binding domain termed MADS-box. Members of the MADS-box family can be classified into two major types: type I, serum response factor (SRF)-like, and type II, myocyte enhancer factor 2 (MEF2)-like (Gramzow and Theissen, 2010), based on sequence specificity in DNA binding, sequence differences and the extent of dissimilarity in DNA binding that they induce (Messenguy and Dubois, 2003; Gramzow and Theissen, 2010). As the first identified member in the MADS family, MCM1 has been shown to be an essential transcription factor that regulates a number of biological processes in fungi, including mini-chromosome maintenance, general metabolism, cell identity, virulence, and pheromone responses by interacting with other cofactors (Messenguy and Dubois, 1993; Mead *et al*., 2002; Yang *et al*., 2015).

In *S. cerevisiae*, homo-dimeric MCM1 activates transcription of a-specific genes in haploid MATa cells. In MATα cells, MCM1 stimulates α-specific gene transcription in the α1-MCM1 complex and blocks a-specific gene expression in complex with α2, which in turn recruits the Ssn6/Tup1 repressor complex (Casselton, 1997; Gavin *et al*., 2000). In the presence of pheromone, STE12, which acts downstream of the MAPK signalling pathway, is recruited in both cell types and associates with MCM1 (in MATa cells), or α1 (in MATα cells) to activate genes required for the pheromone response pathway and cell fusion (Elion *et al*., 1993; Casselton, 2002; Mead *et al*., 2002). In plant pathogenic fungi, MCM1 orthologs seem to be involved in regulating fungal development and pathogenesis. In *M. oryzae*, MoMcm1 interacts with Mst12 and MatA-1 to regulate germ tube identity and male fertility, respectively, and a *Momcm1* deletion mutant is defective in

penetration and forms narrower invasive hyphae leading to reduced virulence (Zhou *et al.*, 2011). Deletion of *FgMcm1* in *Fusarium graminearum* results in a significant reduction in virulence, deoxynivalenol production and conidiation. Interaction of FgMcm1 with Mat1-1-1 or Fst12 also seems to be required for sexual reproduction (Yang *et al.*, 2015). However, in the corn smut fungus, *Ustilago maydis*, deletion of *umc1* leads to an attenuated mating reaction but has no effect on pathogenic development (Krüger *et al.*, 1997). Although the significance of MCM1 in plant pathogenic fungi seems well established, the role of MCM1 in rust fungi remains unknown.

Wheat stripe rust, caused by *Puccinia striiformis* f. sp. *tritici* (*Pst*), is causing huge losses in wheat production worldwide (Zhao *et al.*, 2016). It belongs to the phylum Basidiomycota, which are known for having multiple mating types to govern cell-cell fusion during sexual reproduction (Zheng *et al.*, 2013). *Pst* is an obligate biotrophe and therefore completely dependent on nutrients taken up from the living host through specialized structures, so called haustoria. During the asexual cycle, urediospores continuously infect wheat in repeating cycles throughout the growing season (Garnica *et al.*, 2013), often leading to severe crop losses. Recently, the alternate host on which *Pst* completes its sexual stage was identified to be barberry species (Zhao *et al.*, 2013). The sexual stage was found to contribute majorly to the high degree of virulence diversity in *Pst* (Zheng *et al.*, 2013).

Progress in dissecting mating-related genes in rust fungi has been hampered by their complicated life cycle and the lack of an efficient and stable transformation system. Recently, two allelic homeodomain pairs HD1 (homologs of MATα2 and bE), and HD2 (homologs of MATa1 and bW) (Raudaskoski and Kothe, 2010; Kües *et al.*, 2011), along with three pheromone receptors (STE3) were identified in three *Puccinia* species (Cuomo *et al.*, 2017). *Puccinia triticina* (*Pt*) HD proteins (PtbE1 and PtbW1) can be activated in a heterologous *U. maydis* mating assay, and host-induced gene silencing (HIGS) of the HD and STE3 alleles reduce wheat infections (Bakkeren and Kronstad, 1993; Bakkeren *et al.*, 2008; Cuomo *et al.*, 2017). In addition, the *Ste12* ortholog in *Pst*, *PstSTE12*, can complement a mating defect in the MATα *ste12* mutant of *S. cerevisiae* and participates in regulating virulence of *Pst* (Zhu *et al.*, 2017). These results indicate that mating-related genes may also play an important role in rust pathogenicity. In this study, we found that the *Pst* genome contains two *MCM1* orthologous genes, *PstMCM1-1* and *PstMCM1–2*, and that *PstMCM1-1* is a rust-fungus specific transcription factor. To clarify whether and how *PstMCM1-1* participates in mating and virulence of *Pst*, we performed subcellular localization assays, protein-protein interaction analyses, transcript profiling, complementation of mutants of *S. cerevisiae* and *M. oryzae*, and *PstMCM1-1* knockdown via Barley stripe mosaic virus (BSMV)-mediated HIGS. Our findings indicate that *PstMCM1-1* plays important roles in mating and pathogenicity in *Pst*, and suggest that rust fungi have developed specific *MCM1* genes for adaptation to their hosts during evolution, which identifies them as potential targets for controlling wheat stripe rust.

Results

PstMCM1-1 *is a rust fungus-specific* MCM1 *gene*

A BLAST search using UMC1 from *U. maydis* (Krüger *et al.*, 1997) and MCM1 from *M. oryzae* (Zhou *et al.*, 2011) as queries revealed the presence of two putative MCM1-encoding genes in the genome of the virulent *Pst* isolate CYR32 (Zheng *et al.*, 2013): *PstMCM1-1* and *PstMCM1–2*. *PstMCM1-1* and *PstMCM1–2* encode proteins of 508 and 782 amino acids, respectively, and share 51% sequence identity. They are both SRF-like type transcription factors that contain highly conserved MADS-box motifs in the N-terminal region (Supporting Information Fig. S1A). However, PstMCM1-1 also contains a domain similar to human Epstein-Barr virus (EBV) nuclear antigen 3 (EBNA-3), a nuclear protein important for EBV-induced B-cell immortalization and the immune response to EBV infection (Supporting Information Fig. S1B). In contrast, this domain was not found in PstMCM1–2 (Supporting Information Fig. S1C). Phylogenetic analyses indicated that PstMCM1-1 and PstMCM1–2 fall into two distinct clades (Fig. 1; Supporting Information Table S1). As shown in Fig. 1, all rust fungi seem to contain two putative MCM1 orthologs (light blue shading). One group including PstMCM1–2 can be classified as conventional MCM1, while another group including PstMCM1-1 seems specific to rust fungi (red line). Thus, our results suggest that PstMCM1-1 is a novel MCM1 transcription factor representing a group of MCM1 proteins specific to rust fungi.

PstMCM1-1 *is highly induced during early infection stages of wheat and during pycniospore formation on barberry*

In order to characterize *PstMCM1-1* transcript profiles at different infection stages, quantitative real-time PCR (qRT-PCR) was performed. *PstMCM1-1* transcripts were detected in ungerminated urediospores, infected wheat leaves collected from 6 to 264 hours post inoculation (hpi) and during pycniospore formation in the alternate host, barberry [11 days post inoculation (dpi)]. Values are expressed relative to the endogenous *Pst* reference gene *EF-1*. Up-regulation of *PstMCM1-1* transcripts occurred as soon as the virulent isolate CYR32 encountered leaves of wheat cultivar Suwon11 (Fig. 2). Subsequently, *PstMCM1-1* reached a peak at 12 hpi (more than 25-fold), which corresponds to the time of substomatal vesicle formation.

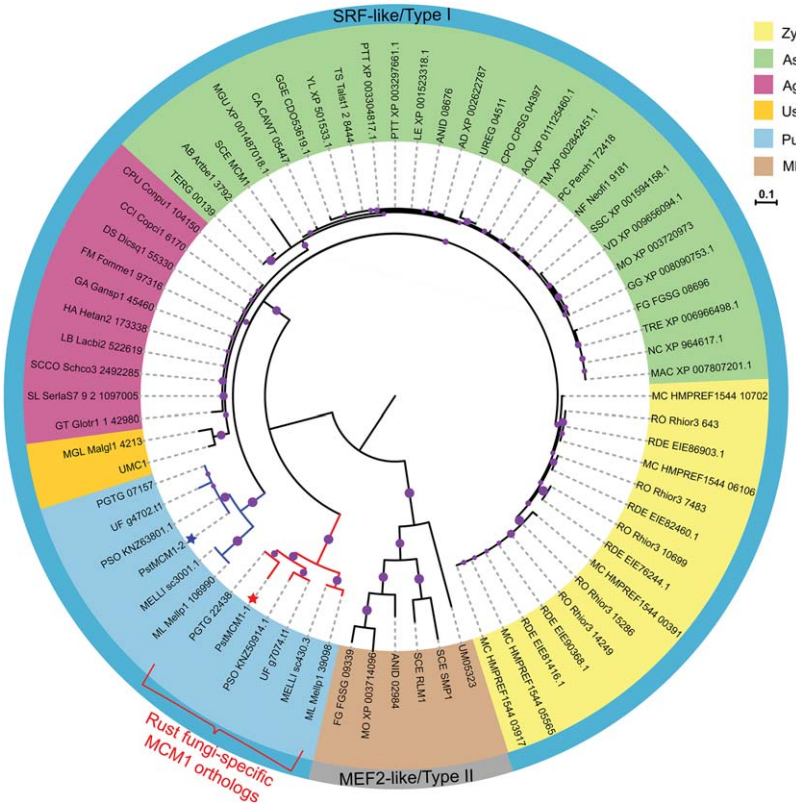

Fig. 1. Phylogeny of fungal MCM1 orthologs. The phylogenetic tree was constructed using the Maximum-likelihood (ML) approach. Scale bars correspond to 0.1 amino acid substitutions. The two subfamilies of MADS-box family members are indicated on the outer circle as SRF-like/Type I, and MEF2-like/type II. The MEF2-like/type II subfamily was used as out-group. PstMCM1-1 and PstMCM1-2 are indicated by red and blue asterisks respectively. For abbreviations, see Supporting Information Table S1.

High expression persists (although declining) until 72 hpi, which is the time initiating successful colonization of the host. Interestingly, *PstMCM1-1* showed a significant up-regulation (87-fold; Fig. 2), during the formation of pycniospore on the alternate host barberry. Transcript profiles of *PstMCM1–2* indicated a peak of expression at 48 hpi (Supporting Information Fig. S2). Expression of *PstMCM1–2* was also induced during pycniospore formation in barberry (Supporting Information Fig. S2).

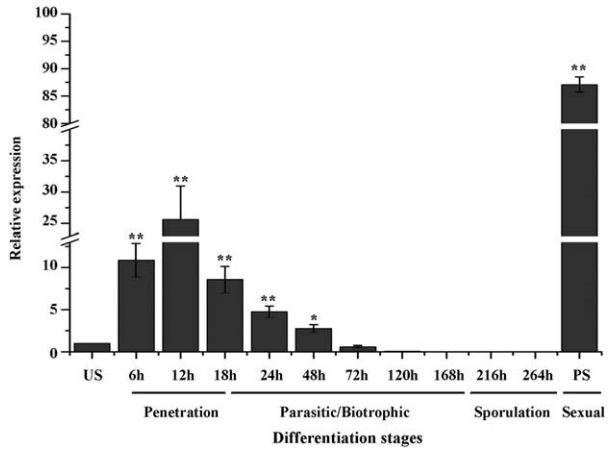

Fig. 2. Transcript profiles of *PstMCM1-1* during *Pst* infection. Relative transcript levels of *PstMCM1-1* were calculated using the $2^{-\Delta\Delta CT}$ method with the endogenous reference gene EF-1 and the values for ungerminated urediospores (US) set to 1. US, urediospores; 6–264 h, 6–264 hpi with CYR32 of wheat; PS, pycniospores on infected *B. shensiana*. Data represent the mean of three biological replicates ± standard errors. Differences were assessed using Student's *t*-tests. Asterisks indicate $P < 0.05$; double asterisks indicate $P < 0.01$.

PstMCM1-1 localizes to the nucleus of plant cells

To determine the subcellular localization of PstMCM1-1, we generated the plasmids pCaMV35S:GFP, and pCaMV35S:PstMCM1-1-GFP and used them for the transformation of wheat protoplasts. The GFP signal was detected in controls throughout cell, including cytoplasm, cytoplasmic membrane and nucleus (Supporting Information Fig. S3). When the PstMCM1-1-GFP fusion protein was transiently expressed in wheat protoplasts, fluorescence was restricted to the nucleus. These data indicate that *PstMCM1-1* localizes to the nucleus of wheat cells.

Yeast two-hybrid assays verify PstSTE12 and PstbE1 as interaction partners of PstMCM1-1

MCM1 is known to interact with other transcription factors to regulate various biological functions in many fungi (Mead *et al.*, 2002; Nolting and Pöggeler, 2006; Zhou *et al.*, 2011; Yang *et al.*, 2015). The predicted protein Pst19228 was found to be an ortholog of PtbE1 (45.48%

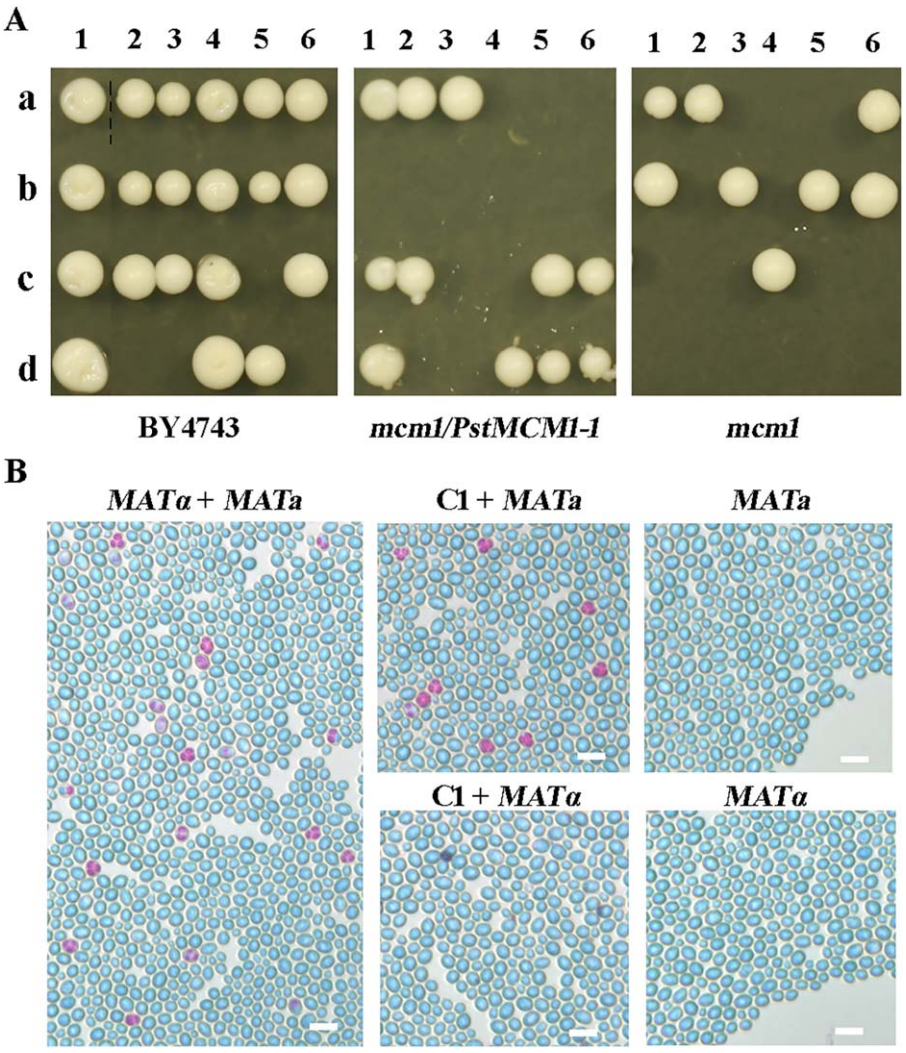

Fig. 3. Complementation of the *S. cerevisiae mcm1* mutant with pDR195-*PstMCM1-1*.
A. Tetrads were dissected from the wild type BY4743, *mcm1* diploid mutants and *mcm1/PstMCM1-1* diploid transformants. Four viable spores (A–D) were obtained from each of the tetrads (lanes 1 and 4) with some exceptions of three-spore tetrads due to random spore inviability in the wild type (lanes 2, 3, 5 and 6). However, only one or two viable spores (lanes 1–6) were obtained from tetrads of the *mcm1* mutant. Three viable spores were obtained from one *mcm1/PstMCM1*-1 diploid transformant (lane 1).
B. Mating is restored by the presence of *PstMCM1-1* in the *S. cerevisiae mcm1* mutant. Ascospores arising through mating are labelled in red. C1, *PstMCM1-1* complemented *mcm1* mutant; MATa and MATα, wild yeast cells of opposite mating types. Bars, 10 μm.

identity; 1.02e-071), and therefore named *PstbE1* (Supporting Information Fig. S4). The predicted HD motifs share high conservation between the two sequences. To verify the interaction between PstMCM1-1 with PstSTE12 and PstbE1, yeast two-hybrid assays were performed. The prey construct of *PstMCM1-1* and bait constructs of *PstSTE12*, or *PstbE1* were co-transformed into yeast strain AH109. Resulting Trp^+ Leu^+ transformants were able to grow on SD-L-W-H-A and displayed LacZ activities similar to the positive control, indicating that PstMCM1-1 is interacting with PstSTE12 and PstbE1 (Supporting Information Fig. S5).

PstMCM1-1 *partially complements* S. cerevisiae mcm1 *mutants*

To test whether *PstMCM1-1* can functionally complement a *S. cerevisiae mcm1* mutant, we transformed pDR195-*PstMCM1-1* into diploid *mcm1*mutants of yeast. Transformants were identified by PCR (Supporting Information Table S2) and cultured on McClary's medium for 5–6 days to generate ascospores. Subsequently, tetrads were separated and grown on YPD medium for 3–5 days. Generally, three or four viable spores could be obtained from tetrads of the wild type, whereas only one to two viable spores were obtained from the *mcm1* mutant, indicating that *MCM1* is an essential gene and disruption of *MCM1* results in a lethal phenotype (Passmore *et al.*, 1988). One transformant with pDR195-*PstMCM1-1* exhibited three viable spores (Fig. 3A, lane 1), while transformants 2–6 have not been complemented. The restore spore was detected as MATα type by PCR (data not shown), termed C1. This result shows that spore viability of the *mcm1* mutant can at least partially be complemented by *PstMCM1-1*.

As shown in Fig. 3B, *PstMCM1-1* in the transformant C1 is also capable to restore mating in the *S. cerevisiae mcm1* mutant. This result might be taken as evidence that *PstMCM1-1* might also play a role in sexual reproduction in *Pst*.

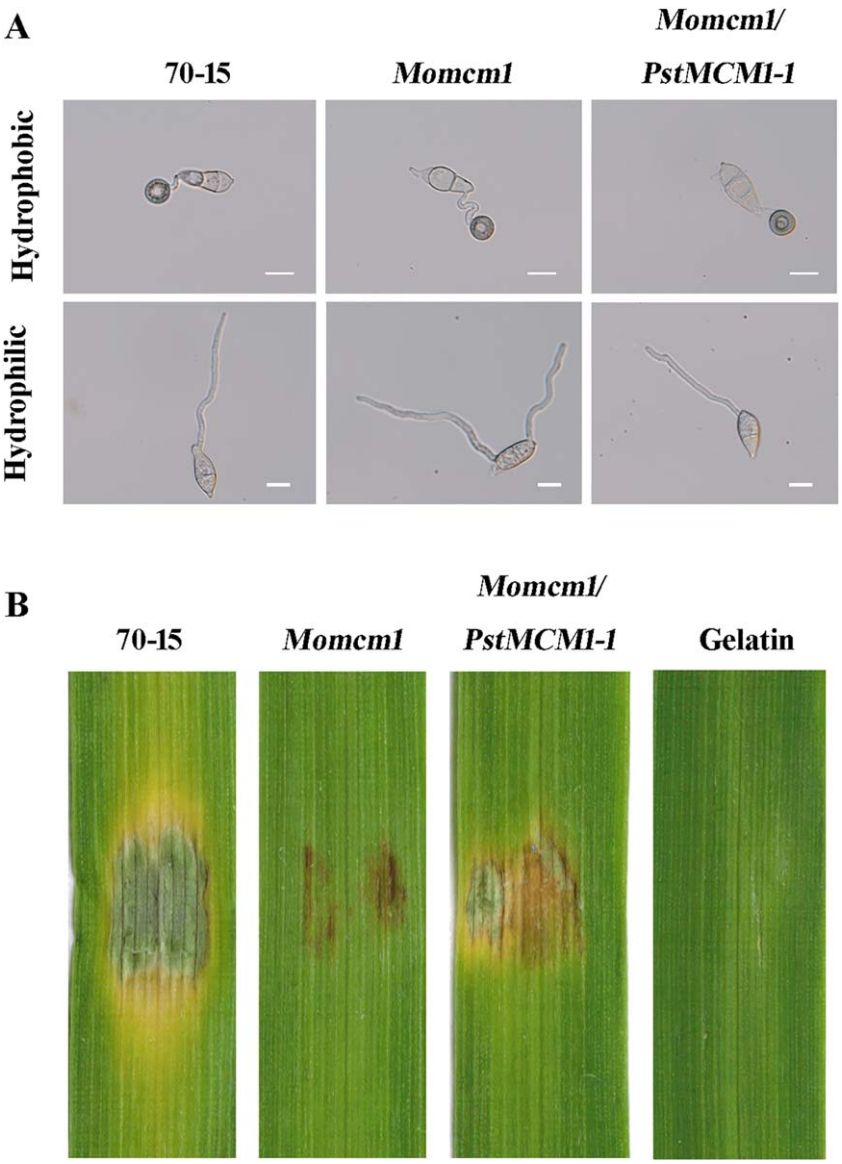

Fig. 4. Complementation of the *Momcm1* mutant of *M. oryzae* with *PstMCM1-1*.
A. Appressorium formation assays on hydrophobic and hydrophilic surfaces. Appressoria are formed by the wild type 70–15 and the *Momcm1* mutant on hydrophobic but not the hydrophilic surfaces after 24 h. The mutant produced long curved germ tubes on both surfaces, while the wild type and the *PstMCM1-1* transformants formed normal appressoria. Bars, 10 μm.
B. Barley infection assay. From left to right, barley leaves inoculated with conidia of the wild type (70–15), the *Momcm1* mutant, the *PstMCM1-1* transformant, and 0.25% gelatin (control). Typical phenotypes were photographed at 6 dpi.

PstMCM1-1 *partially complements* Momcm1 *in* M. oryzae *mutants*

We heterologously expressed *PstMCM1-1* under the control of the RP27 promoter (derived from the *M. oryzae* ribosomal protein 27 gene) in a *Momcm1* mutant. Geneticin-resistant transformants were isolated and verified by PCR. On artificial hydrophobic surfaces, about 80% of mutant conidia formed appressoria by 24 h (Supporting Information Table S3). Under the same conditions, over 93% conidia of the wild-type strain 70–15 and over 87% of complemented conidia formed appressoria. Mature appressoria formed by the mutant, 70–15 and transformants all had normal size, morphology and melanization. Over 56% of *Momcm1* germ tubes were curved and tended to be longer than those of the wild type (Fig. 4A; Supporting Information Table S3). However, the majority (over 80%) of germ tubes of *PstMCM1-1* transformants were normal and short as the wild type (Fig. 4A; Supporting Information Table S3). On hydrophilic surfaces, wild type, *Momcm1* mutant, and *PstMCM1-1* transformants did not form appressoria. However, unlike the curved, wider germ tubes produced by the *Momcm1* mutant, *PstMCM1-1* transformants usually formed straight, long germ tubes as the wild type (Fig. 4A; Supporting Information Table S3).

In order to determine whether *PstMCM1-1* could complement the defects of the *M. oryzae* mutant in plant infection, 8-day-old barley seedlings of cultivar NB6 were drop inoculated with conidia. At 6 dpi, leaves inoculated with the wild type developed typical blast lesions (Fig. 4B). No lesions were observed on leaves inoculated with gelatin (control), while only small lesions were observed on leaves

inoculated with conidia of the *Momcm1* mutant (Fig. 4B). Under the same conditions, *PstMCM1-1* transformants caused more and larger lesions on barley leaves. These results indicated that *PstMCM1-1* could complement the *mcm1* mutant in appressorium formation and plant infection.

Silencing of PstMCM1-1 *reduces virulence of* Pst *on wheat*

BSMV-HIGS was used to further characterize the function of *PstMCM1-1* during the interaction between wheat and *Pst*. Two approximately 250-bp silencing segments of *PstMCM1-1* derived from the 5′-prime and the 3′-end of the gene were selected for silencing of the *PstMCM1-1* gene, named BSMV:*PstMCM1-1*-H and BSMV:*PsMCM1-1*-B (Supporting Information Fig. S6; Supporting Information Table S2). All BSMV-inoculated plants displayed mild chlorotic mosaic symptoms at 10 dpi (Fig. 5A). The fourth leaf was then inoculated with fresh urediospores of *Pst* isolate CYR32 on mock-inoculated plants and leaves that were previously infected with BSMV:γ (the control), BSMV:*PstMCM1-1-H*, and BSMV:*PstMCM1-1-B* respectively (Fig. 5B). Fewer fungal uredia were observed on leaves infected with *BSMV:PstMCM1-1-H* and *BSMV:PstMCM1-1-B* (Fig. 5B and F). In contrast, leaves infected with BSMV:γ and inoculated with CYR32 produced numerous urediospores (Fig. 5B and F). Compared with transcript levels in leaves inoculated with BSMV:γ, expression of *PstMCM1-1* was reduced down by 72% and 70% in leaves pre-inoculated with BSMV:*PstMCM1-1-H* at 48 and 120 hpi with CYR32 respectively (Fig. 5C). Similarly, in leaves pre-inoculated with BSMV:*PstMCM1-1-B*, transcripts of *PstMCM1-1* were reduced by 75% and 58% at 48 and 120 hpi with CYR32 respectively (Fig. 5C). In addition, expression of *PstSTE12* and *PstbE1* in *PstMCM1-1* silenced plants were suppressed (Fig. 5D and E). However, the expression of some defense-related genes in wheat was induced in *PstMCM1-1*-silenced plants at least at 120 hpi (Supporting Information Fig. S7). The number of uredia on wheat leaves inoculated with BSMV:*PstMCM1-1*-H, or BSMV:*PstMCM1-1*-B was significantly reduced in *PstMCM1-1*-silenced plants at 14 dpi (Fig. 5F). These results indicate that the silencing of *PstMCM1-1* increases wheat resistance against *Pst* and that *PstMCM1-1* contributes to *Pst* virulence in wheat.

Silencing of PstMCM1-1 *suppresses fungal growth during* Pst-*wheat interaction*

To determine how *PstMCM1-1* affects *Pst* pathogenicity, we analyzed cytological changes in *PstMCM1-1*-silenced plants inoculated with *Pst* CYR32 at 48 hpi, the number of haustorial mother cells, indicating fungal penetration, and infection hyphal length, indicating the expansion abilities, were reduced compared with BSMV:γ-treated leaves (Fig. 6A, C and D). The number of hyphal branches was not significantly different from the control at 48 hpi (Fig. 6D). At 120 hpi with CYR32, control plants (BSMV:γ) showed extensive colonization and abundant secondary hyphae formation (Fig. 6B and E). In contrast, in *PstMCM1-1*-silenced plants hyphal growth was significantly reduced (Fig. 6B and E). These results indicate that *PstMCM1-1* most likely contributes to fungal growth by participating in hyphal development in *Pst*. Thus, *PstMCM1-1* may also be involved in rust invasion and pathogenicity.

Discussion

MCM1 seems to play crucial roles in regulating a wide range of biological processes. In the present study, we identified two putative *MCM1* genes in the *Pst* genome, *PstMCM1-1* and *PstMCM1–2*, and functionally characterized *PstMCM1-1*. From the phylogenetic analysis, we found that all rust fungi have two putative MCM1 orthologs and PstMCM1-1 was identified as a rust-specific MCM1 ortholog. Basidiomycetes usually have multiple mating types and a life cycle in which mating, cell fusion and nuclear fusion are partitioned by a variable period of vegetative growth (Casselton, 2002). *U. maydis* as a model basidiomycete has been found to possess nearly 50 different mating types (Banuett, 1995). In addition, in *S. cerevisiae*, MCM1 plays a key role in regulating the cell type by interacting with the a1 or α1, α2 proteins (Smith and Johnson, 1992; Mead *et al.*, 2002). We speculate that the two *Pst* MCM1 orthologs may contribute to different development stages and the multiple mating types in *Pst*. In our heterologous complementation assay, when introducing *PstMCM1-1* into a wild-type diploid yeast mutant, the lethal phenotype of a yeast *mcm1* mutation was partially complemented. Subsequent mating assays showed that the fertility of the mutant was also restored. Similar to MCM1 from *S. cerevisiae*, *PstMCM1-1* also contains highly conserved MADS-box motifs in its N-terminal region. Due to its structural and functional similarity with MCM1 from *S. cerevisiae*, it is likely that *PstMCM1-1* plays a role in the regulating the mating process in *Pst*. In addition, *PstMCM1-1* was also highly up-regulated (80-fold) on barberry, which is the alternate host on which sexual reproduction results in pycniospore production (Jin *et al.*, 2010; Zhao *et al.*, 2013). Thus, our data strongly suggest that *PstMCM1-1* contributes to sexual reproduction in *Pst*.

Previous studies demonstrated that MCM1 participates in biological functions via interacting with several regulatory proteins and co-factors (Mead *et al.*, 2002; Fornara *et al.*, 2003; Nolting and Pöggeler, 2006). Our yeast two-hybrid screen identified *PstSTE12* and *PstbE1* as

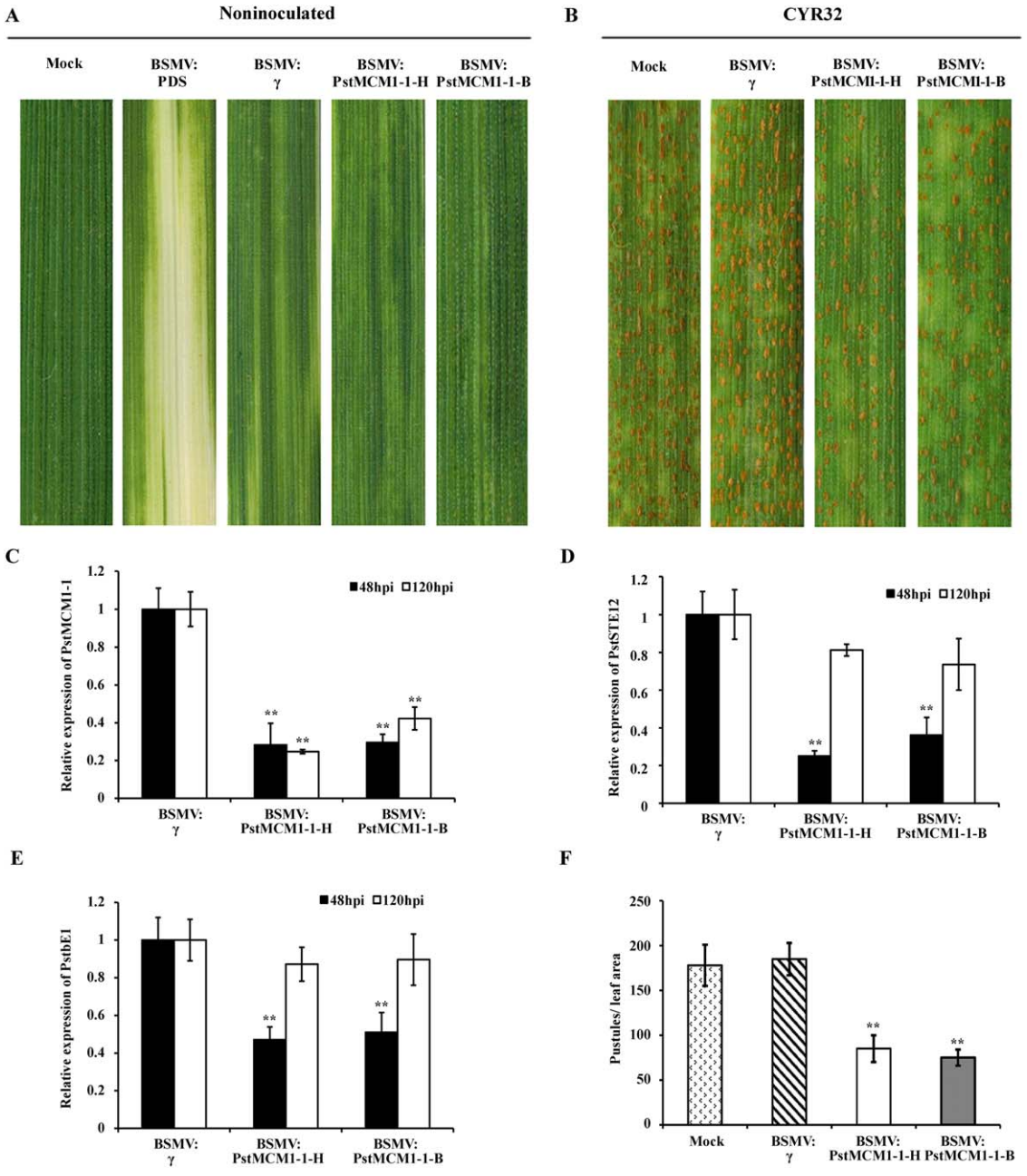

Fig. 5. Silencing of *PstMCM1-1* leads to reduced virulence of *Pst* on wheat.

A. No change of phenotype was observed in wheat leaves mock-inoculated with FES buffer (Mock). Mild chlorotic mosaic symptoms were observed in wheat leaves inoculated with BSMV:γ (control), BSMV:*PstMCM1-1*-H and BSMV:*PstMCM1-1*-B. Photobleaching was evident on wheat leaves infected with BSMV:*TaPDS* as control.

B. Phenotypes of the fourth leaf of wheat plants inoculated with FES buffer (Mock), BSMV:γ (control), BSMV:*PstMCM1-1*-H and BSMV:*PstMCM1-1*-B at 14 dpi with the virulent *Pst* isolate CYR32.

C. Relative transcript levels of *PstMCM1-1* in *PstMCM1-1*-knockdown wheat leaves. RNA samples were isolated from the fourth leaf of wheat infected with BSMV:γ, BSMV:*PstMCM1-1*-H and BSMV:*PstMCM1-1*-B at 48 and 120 hpi with the virulent CYR32 isolate. Values are expressed relative to an endogenous *Pst* reference *EF1* gene, with the empty vector (BSMV:γ) set to 1.

D. Relative transcript levels of *PstSTE12* in *PstMCM1-1*-knockdown wheat leaves at 48 and 120 hpi.

E. Relative transcript levels of *PstbE1* in *PstMCM1-1*-knockdown wheat leaves at 48 and 120 hpi.

F. Quantification of uredinial density in *PstMCM1-1*-knockdown plants at 14 dpi with the virulent *Pst* isolate. Values represent mean ± standard errors of three independent assays. Differences were assessed using Student's *t*-tests. Double asterisks indicate $P < 0.01$.

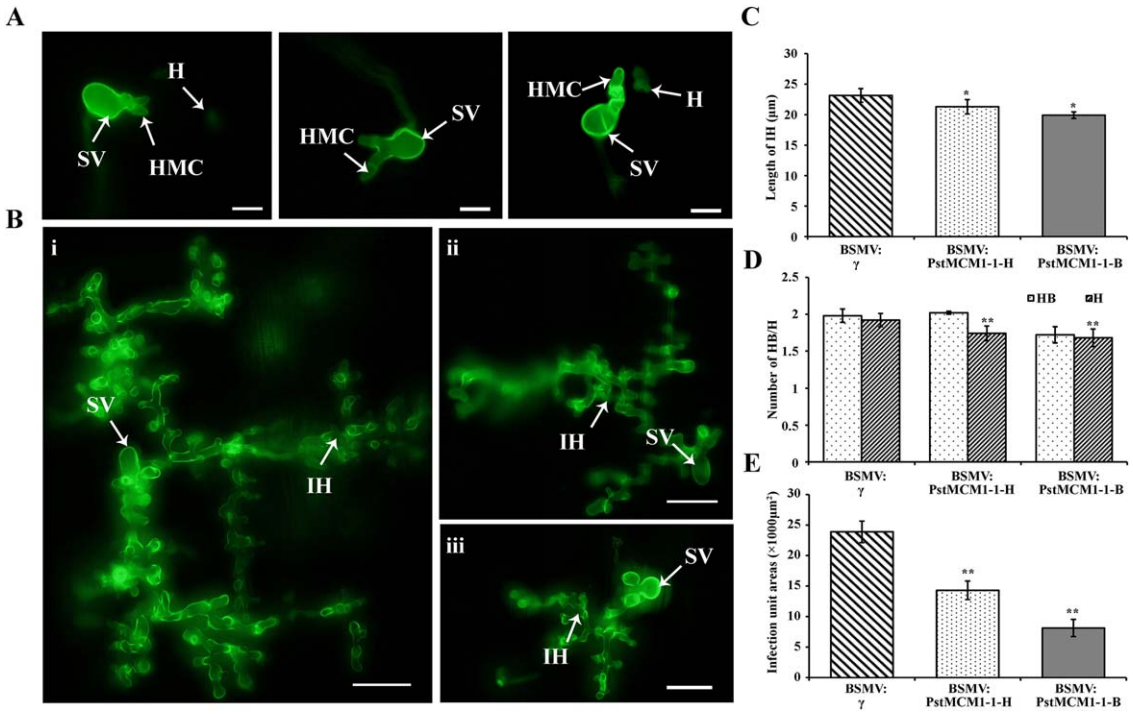

Fig. 6. Histological observation of fungal growth in wheat infected by BSMV:γ and recombinant BSMV after inoculation with virulent CYR32.
A. Fungal growth at 48 hpi (from left to right) in BSMV:γ-infected plants, BSMV:*PstMCM1-1*-H-infected plants and BSMV:*PstMCM1-1*-B-infected plants.
B. Fungal growth at 120 hpi in (i) BSMV:γ-infected plants, (ii) BSMV:*PstMCM1-1*-H-infected plants and (iii) BSMV:*PstMCM1-1*-B-infected plants.
C. Significant decrease in the length of infection hyphae (IH) in *PstMCM1-1*-silenced plants at 48 hpi with CYR32.
D. A significant decrease in the number of haustoria (H) but no significant difference in the number of branches of IH per infection unit were observed between control and *PstMCM1-1*-silenced plants.
E. The infection unit area at 120 hpi was significantly decreased in *PstMCM1-1*-silenced plants inoculated with CYR32. Values represent the means ± standard errors of three independent samples. Differences were assessed using Student's *t*-tests. Asterisks indicate $P < 0.05$, double asterisks indicate $P < 0.01$. SV, substomatal vesicle; SH, secondary hypha; IH, infection hypha; HMC, haustorial mother cell; H, haustorium; HB, hyphal branch.

interaction partners of *PstMCM1-1*. In *S. cerevisiae*, Ste12 is a key transcription factor downstream of MAPK pathways involved in mating and control of filamentous growth (Madhani and Fink, 1997; Rispail and Pietro, 2010). The interaction of MCM1 with Mat or Ste12 proteins has been shown to be important for sexual reproduction in various pathogens (Zhou *et al*., 2011; Yang *et al*., 2015). Thus, PstMCM1-1 may interact with PstSTE12 to exert its effect on fungal cellular functions through its role in the MAPK pathway. In addition, blast analysis showed that *PstbE1* encodes a HD2-containing protein. Given the fact that we found two MCM1 orthologs in *Pst* and that we were able to show an interaction between PstMCM1-1 and PstbE1, it is likely that *Pst* possesses a more complicated mating type system. Recently, genome analysis demonstrated that the proposed simple ± bipolar system is more complex in cereal rust fungi (Cuomo *et al*., 2017). The redundancy of MCM1 proteins may have resulted in *Puccinia* lineage-specific adaptations and the interactions between PstMCM1-1 and PstSTE12, or PstbE1 provide evidence that they may play important roles in forming a complex, as demonstrated for *M. oryzae*, where the interaction of MoMcm1 with Mst12 and MatA-1 is regulating germ tube identity and male fertility respectively (Zhou *et al*., 2011).

In plant pathogens, the role of MCM1 orthologs in pathogenesis varies between different species. In *U. maydis*, MCM1 is dispensable for virulence (Messenguy and Dubois, 2003). In contrast, *MoMCM1* is important for virulence in *M. oryzae*, and *Momcm1* mutants form abnormal and long germ tubes and were less aggressive on rice and barley (Zhou *et al*., 2011). In our study, expression of *PstMCM1-1* in the *Momcm1* mutant partially restored the formation of normal germ tubes and virulence. MCM1s seem to be functionally conserved between *M. oryzae* and *Pst*, which provides additional evidence that *PstMCM1-1* may be involved in infection and virulence in *Pst*. In addition, the high expression level of *PstMCM1-1* during early *Pst* infection, may also indicate a possible function in

asexual development. Silencing of *PstMCM1-1* via BSMV-HIGS further verified the function of this gene as an important pathogenicity factor. Phenotypic and cytological observations indicate that silencing of *PstMCM1-1* results in a restriction of haustorium formation for primary infection and hyphal development for further extension. Taken together, this significantly limits uredia generation on wheat leaves. Notably, the decreased transcript levels of *PstSTE12* and *PstbE1* after silencing of *PstMCM1-1* suggests that the both genes are affected by the expression of *PstMCM1-1*, and that *PstMCM1-1* might play a role in regulating virulence via regulation of the two cofactors.

In general, *PstMCM1-1*, in interaction with cofactors, can contribute to virulence by regulating haustorium formation for fungal colonization and further development, and thus may be considered an important pathogenesis factor. Our research on *PstMCM1-1* provides the basis for further exploration into virulence regulation and mating processes in *Pst*.

Materials and methods

RNA isolation and qRT-PCR analysis

Wheat leaves were sampled at 6, 12, 18, 24, 36, 48, 72, 120, 168, 216 and 264 hpi during the interaction of the virulent *Pst* race CYR32 and the susceptible wheat cultivar Suwon 11 (Su11), and at 11 dpi from barberry leaves infected by CYR32 basidiospores. Total RNA was extracted with the Qiagen Plant RNeasy kit (Qiagen, Hilden, Germany). cDNA was synthesized with the RevertAid First Strand cDNA Synthesis Kit (Thermo Fisher Scientific, Waltham, MA). The primer pair RT-PstMCM1-1-F/R (Supporting Information Table S2) was selected to perform qRT-PCR on a CFX Connect Real-Time System (Bio-Rad, Hercules, CA), with *PstEF1* as internal control (Guo *et al*., 2011). PCR conditions were as described previously (Cheng *et al*., 2016). Relative transcript levels were calculated using the $2^{-\Delta\Delta CT}$ method (Livak and Schmittgen, 2001) using three biological replicates.

Sequence alignments and phylogenetic analysis

MCM1 homologs of *Pst* and other proteins were identified by Blastp searches using NCBI (http://www.ncbi.nlm.nih.gov/). A cut off of less than e^{-5} was used. Conserved domains of putative proteins were determined using HMMER 3.0 (http://hmmer.org/). MEGA5 was used to generate phylogenetic trees (Tamura *et al*., 2011). Multiple sequence alignments were performed using ClustalW version 1.8 (Thompson *et al*., 1994), and shading was added using Boxshade online (http://www.ch.embnet.org/software/BOX_form.html).

Yeast two-hybrid assay

The prey construct of *PSTMCM1-1* was generated by cloning the *Pst* cDNA fragment amplified with primer pair AD-MCM1-1-F/R (Supporting Information Table S2) into pGAKT7 (Clontech, Mountain View, CA). Bait constructs of *PstSTE12* and *PstbE1* were generated by cloning cDNA fragment amplified with primer pairs BD-PstSTE12-F/R and BD-PstbE1-F/R (Supporting Information Table S2) into pGBDT7 (Clontech) respectively. After confirmation by sequence analysis, bait and prey constructs were transformed in pairs into yeast strain AH109. Trp^+ and Leu^+ yeast transformants were isolated and assayed for growth on SD-Trp-Leu-His-Ade medium and LacZ activities. A haemocytometer was used to dilute the density to 10^7, 10^6, 10^5 and 10^4 cells ml^{-1}. 3-Amino-1,2,4-triazole (3-AT) was added to a final concentration of 3 mM to inhibit activation of transcription factor *Pst*STE12.

Complementation of S. cerevisiae mcm1 *(MATα) mutants*

The *Saccharomyces cerevisiae* diploid mutant strain BY4743 (*MATa/MATα*; *ura3Δ0/ura3Δ0*; *leu2Δ0/leu2Δ0*; *his3Δ1/his3Δ1*; *met15Δ0/MET15*; *LYS2/lys2Δ0*; *YMR043w/YMR043w*::*kanMX4*) was purchased from EUROSCARF (Frankfurt, Germany). The strain was transformed with pDR195-*PstMCM1-1* using the lithium acetate method as described in the operation manual (Clontech, Japan). Transformants were selected on minimal medium lacking uracil but supplemented with all amino acids and screened by PCR using the primer pair pDR195-MCM1-1-F/R (Supporting Information Table S2). Transformants were cultured overnight in YPD, and tetrads were dissected from sporulating transformants under a MSM400 dissection microscope (Singer Instruments, Roadwater, The United Kingdom) (Bloom *et al*., 2013), after plating on McClary's medium at 30°C for 5–7 days. Three days later, arrested spores were recovered, and the mating type of spores that showed G418 resistance was identified as *MATα* by PCR (Data not shown). After 4 days, cells were fixed with phenol and methylene blue as described (Lanchun *et al*., 2003). Ascospores were stained with phenol red.

Complementation of the M. oryzae *null-mutant* mcm1 *by* PstMCM1-1

The PCR fragment of *PstMCM1-1* amplified with primers pFL2-MCM1-1-F/R (Supporting Information Table S2) was co-transformed with the *Xho*I-digested pFL2 vector into *S. cerevisiae* strain XK1–25 to obtain pFL2-*PstMCM1-1*. pFL2-*PstMCM1-1* was transformed into protoplasts of the *M. oryzae mcm1* mutant. Transformants were verified by geneticin resistance and PCR to confirm insertion of *PstMCM1-1* into the *M. oryzae* genome. Appressorium formation was assayed as described (Hara *et al*., 2005). For plant infection assays, conidia were resuspended to 10^5 conidia/ml in sterile distilled water, and then spotted onto leaves of 8-day-old barley seedlings (Zhang *et al*., 2016). Lesion formation was examined 6 dpi.

BSMV-mediated HIGS of PstMCM1-1

Two cDNA fragments were used to silence *PstMCM1-1* (Supporting Information Fig. S6; Supporting Information Table S2). BLAST analyses showed that the fragments were specific with no similarity to wheat genes. Capped *in vitro* transcripts were prepared from linearized plasmids containing the tripartite BSMV genome (Petty *et al*., 1990) using the RiboMAX TM

Large-Scale RNA Production System-T7 (Promega, Madison, WI, USA) and the Ribom^{7}G Cap Analog (Promega), according to the manufacturer's instructions. The second leaf of a two-leaf wheat seedling was inoculated with BSMV transcripts and incubated at 25°C. BSMV:*TaPDS* was used as a positive control to confirm the success of inoculation (Holzberg *et al*., 2002). Leaves were photographed after 10 days. The fourth leaves were inoculated with CYR32 and sampled at 48 and 120 hpi for RNA isolation and cytological observation. Wheat phenotypes after *Pst* inoculation were recorded and photographed at 14 dpi. The experiment was repeated at least three times.

Histological observations of fungal growth

Wheat leaves infected with BSMV were sampled at 48 and 120 hpi with *Pst* and stained (Cheng *et al*., 2015). Inoculated leaves were excised and then fixed and decolorized in ethanol/trichloromethane (3:1 v/v) containing 0.15% (w/v) trichloroacetic acid for 3–5 days. Specimens were immersed in saturated chloral hydrate until the leaf tissue became translucent and then stained with wheat germ agglutinin conjugated to Alexa-488 (Invitrogen, Waltham, MA) as described (Ayliffe *et al*., 2011). For each sample, 30–50 infection sites from three leaves were examined to assess the number of haustoria and hyphal branches, hyphal length and infection area. All microscopic assays were performed with an Olympus BX-51 microscope (Olympus, Tokyo, Japan).

Subcellular localization analysis

The subcellular localization of *PstMCM1-1* was determined in wheat protoplasts. Su11 plants for protoplast transformation were cultivated in the glasshouse for 2–3 weeks. Plasmid pCaMV35S:*PstMCM1-GFP* and the control plasmid pCaMV35S:*GFP* were separately transformed into wheat protoplasts through polyethyleneglycol (PEG)-calcium transfection (Yoo *et al*., 2007). After culturing for 18–24 h, GFP signals in transformed protoplasts were observed with a fluorescence microscope (Olympus BX-51).

Acknowledgements

This study was supported by the National Natural Science Foundation of China (No. 31371889 and 31620103913), the National Basic Research Program of China (No. 2013CB127700), and the 111 Project from the Ministry of Education of China (No. B07049). The authors thank Dr. Jinqiu Zhou from Institute of Biochemistry and Cell Biology, SIBS, CAS, China for providing technical supports on tetrad separation of yeast, and Dr. Larry Dunkle from the USDA-Agricultural Research Service at Purdue University, USA for critical reading the manuscript.

References

Ayliffe, M., Devilla, R., Mago, R., White, R., Talbot, M., Pryor, A., and Leung, H. (2011) Nonhost resistance of rice to rust pathogens. *Mol Plant Microbe Interact* **24:** 1143–1155.

Bakkeren, G., and Kronstad, J.W. (1993) Conservation of the b mating-type gene complex among bipolar and tetrapolar smut fungi. *Plant Cell* **5:** 123–136.

Bakkeren, G., Kämper, J., and Schirawski, J. (2008) Sex in smut fungi: structure, function and evolution of mating-type complexes. *Fungal Genet Biol* **45:** S15–S21.

Banuett, F. (1995) Genetics of *Ustilago maydis*, a fungal pathogen that induces tumors in maize. *Annu Rev Genet* **29:** 179–208.

Bloom, J.S., Ehrenreich, I.M., Loo, W.T., Lite, T.L., and Kruglyak, L. (2013) Finding the sources of missing heritability in a yeast cross. *Nature* **494:** 234–237.

Casselton, L.A. (1997) Molecular recognition in fungal mating. *Endeavour* **21:** 159.

Casselton, L.A. (2002) Mate recognition in fungi. *Heredity* **88:** 142.

Cheng, Y., Wang, X., Yao, J., Voegele, R.T., Zhang, Y., Wang, W., *et al*. (2015) Characterization of protein kinase *PsSRPKL*, a novel pathogenicity factor in the wheat stripe rust fungus. *Environ Microbiol* **17:** 2601–2617.

Cheng, Y., Wang, W., Yao, J., Huang, L., Voegele, R.T., Wang, X., and Kang, Z. (2016) Two distinct Ras genes from *Puccinia striiformis* exhibit differential roles in rust pathogenicity and cell death. *Environ Microbiol* **18:** 3910–3922.

Cuomo, C.A., Bakkeren, G., Khalil, H.B., Panwar, V., Joly, D., Linning, R., *et al*. (2017) Comparative analysis highlights variable genome content of wheat rusts and divergence of the mating loci. *G3 Genes Genom Genet* **7:** 361–376.

Elion, E.A., Satterberg, B., and Kranz, J.E. (1993) FUS3 phosphorylates multiple components of the mating signal transduction cascade: evidence for STE12 and FAR1. *Mol Biol Cell* **4:** 495–510.

Fornara, F., Marziani, G., Mizzi, L., Kater, M., and Colombo, L. (2003) MADS-Box genes controlling flower development in rice. *Plant Biol* **5:** 16–22.

Garnica, D.P., Upadhyaya, N.M., Dodds, P.N., Rathjen, J.P., and Matz, M.V. (2013) Strategies for wheat stripe rust pathogenicity identified by transcriptome sequencing. *PLoS One* **8:** e67150.

Gavin, I.M., Kladde, M.P., and Simpson, R.T. (2000) Tup1p represses Mcm1p transcriptional activation and chromatin remodeling of an a-cell-specific gene. *Embo J* **19:** 5875–5883.

Gramzow, L., and Theissen, G. (2010) A hitchhiker's guide to the MADS world of plants. *Genome Biol* **11:** 214–211.

Guo, J., Dai, X., Xu, J.-R., Wang, Y., Bai, P., Liu, F., *et al*. (2011) Molecular characterization of a Fus3/Kss1 type MAPK from *Puccinia striiformis* f. sp. *tritici*, *Ps*MAPK1. *PloS One* **6:** e21895.

Hara, T., Itoh, K., Tanaka, N., and Kudo, Y. (2005) A mitogen-activated protein kinase cascade regulating infection-related morphogenesis in *Magnaporthe grisea*. *Plant Cell* **17:** 1317–1329.

Holzberg, S., Brosio, P., Gross, C., and Pogue, G.P. (2002) Barley stripe mosaic virus-induced gene silencing in a monocot plant. *Plant J* **30:** 315–327.

Jin, Y., Szabo, L.J., and Carson, M. (2010) Century-old mystery of *Puccinia striiformis* life history solved with the identification of *Berberis* as an alternate host. *Phytopathology* **100:** 432–435.

Krüger, J., Aichinger, C., Kahmann, R., and Bölker, M. (1997) A MADS-box homologue in *Ustilago maydis* regulates the expression of pheromone-inducible genes but is nonessential. *Genetics* **147:** 1643–1652.

Kües, U., James, T.Y., and Heitman, J. (2011) Mating type in basidiomycetes: unipolar, bipolar, and tetrapolar patterns of sexuality. In *The Mycota, Evolution of Fungi and Fungal-like Organisms*. Pöggeler, S., and Wöstemeyer, J. (eds). Berlin: Springer-Verlag, pp. 97–160.

Lanchun, S., Bochu, W., Liancai, Z., Jie, L., Yanhong, Y., and Chuanren, D. (2003) The influence of low-intensity ultrasonic on some physiological characteristics of *Saccharomyces cerevisiae*. *Colloids Surf B Biointerfaces* **30:** 61–66.

Livak, K.J., and Schmittgen, T.D. (2001) Analysis of relative gene expression data using real-time quantitative PCR and the $2_T^{-\Delta\Delta C}$ method. *Methods* **25:** 402–408.

Madhani, H.D., and Fink, G.R. (1997) Combinatorial control required for the specificity of yeast MAPK signaling. *Science* **275:** 1314–1317.

Mead, J., Bruning, A.R., Gill, M.K., Steiner, A.M., Acton, T.B., and Vershon, A.K. (2002) Interactions of the Mcm1 MADS box protein with cofactors that regulate mating in yeast. *Mol Cell Biol* **22:** 4607–4621.

Messenguy, F., and Dubois, E. (1993) Genetic evidence for a role for MCM1 in the regulation of arginine metabolism in *Saccharomyces cerevisiae*. *Mol Cell Biol* **13:** 2586–2592.

Messenguy, F., and Dubois, E. (2003) Role of MADS box proteins and their cofactors in combinatorial control of gene expression and cell development. *Gene* **316:** 1–21.

Nolting, N., and Pöggeler, S. (2006) A STE12 homologue of the homothallic ascomycete *Sordaria macrospora* interacts with the MADS box protein MCM1 and is required for ascosporogenesis. *Mol Microbiol* **62:** 853–868.

Passmore, S., Maine, G.T., Elble, R., Christ, C., and Tye, B.K. (1988) *Saccharomyces cerevisiae* protein involved in plasmid maintenance is necessary for mating of MAT alpha cells. *J Mol Biol* **204:** 593–606.

Petty, I.T., French, R., Jones, R.W., and Jackson, A.O. (1990) Identification of barley stripe mosaic virus genes involved in viral RNA replication and systemic movement. *Embo J* **9:** 3453–3457.

Raudaskoski, M., and Kothe, E. (2010) Basidiomycete mating type genes and pheromone signaling. *Eukaryot Cell* **9:** 847–859.

Rispail, N., and Pietro, A.D. (2010) The homeodomain transcription factor Ste12. *Commun Integr Biol* **3:** 327–332.

Shore, P., and Sharrocks, A.D. (1995) The MADS-box family of transcription factors. *Eur J Biochem* **229:** 1–13.

Smith, D.L., and Johnson, A.D. (1992) A molecular mechanism for combinatorial control in yeast: MCM1 protein sets the spacing and orientation of the homeodomains of an α2 dimer. *Cell* **68:** 133–142.

Tamura, K., Peterson, D., Peterson, N., Stecher, G., Nei, M., and Kumar, S. (2011) MEGA5: molecular evolutionary genetics analysis using maximum likelihood, evolutionary distance, and maximum parsimony methods. *Mol Biol Evol* **28:** 2731–2739.

Thompson, J.D., Higgins, D.G., and Gibson, T.J. (1994) CLUSTAL W: improving the sensitivity of progressive multiple sequence alignment through sequence weighting, position-specific gap penalties and weight matrix choice. *Nucleic Acids Res* **22:** 4673–4680.

Yang, C., Liu, H., Li, G., Liu, M., Yun, Y., Wang, C., *et al.* (2015) The MADS-box transcription factor FgMcm1 regulates cell identity and fungal development in *Fusarium graminearum*. *Environ Microbiol* **17:** 2762–2776.

Yoo, S.-D., Cho, Y.-H., and Sheen, J. (2007) Arabidopsis mesophyll protoplasts: a versatile cell system for transient gene expression analysis. *Nat Protoc* **2:** 1565–1572.

Zhang, S.J., Jiang, C., Zhang, Q., Qi, L.L., Li, C.H., and Xu, J.R. (2016) Thioredoxins are involved in the activation of the *PMK1* MAP kinase pathway during appressorium penetration and invasive growth in *Magnaporthe oryzae*. *Environ Microbiol* **18:** 3768–3784.

Zhao, J., Wang, L., Wang, Z., Chen, X., Zhang, H., Yao, J., *et al.* (2013) Identification of eighteen *Berberis* species as alternate hosts of *Puccinia striiformis* f. sp. *tritici* and virulence variation in the pathogen isolates from natural infection of barberry plants in China. *Phytopathology* **103:** 927–934.

Zhao, J., Wang, M., Chen, X., and Kang, Z. (2016) Role of alternate hosts in epidemiology and pathogen variation of cereal rusts. *Annu Rev Phytopathol* **54:** 207–228.

Zheng, W., Huang, L., Huang, J., Wang, X., Chen, X., Zhao, J., *et al.* (2013) High genome heterozygosity and endemic genetic recombination in the wheat stripe rust fungus. *Nat Commun* **4:** 2673–2682.

Zhou, X., Liu, W., Wang, C., Xu, Q., Wang, Y., Ding, S., and Xu, J.R. (2011) A MADS-box transcription factor MoMcm1 is required for male fertility, microconidium production and virulence in *Magnaporthe oryzae*. *Mol Microbiol* **80:** 33–53.

Zhu, X.G., Liu, W., Chu, X.L., Sun, Q.X., Tan, C.L., Yang, Q., *et al.* (2017) The transcription factor *PstSTE12* is required for virulence of *Puccinia striiformis* f. sp. *tritici*. *Mol Plant Pathol.* doi: 10.1111/mpp.12582.

Supporting information

Additional Supporting Information may be found in the online version of this article at the publisher's web-site:

Fig. S1. Sequence analysis of MADS-box motifs. (A) Sequence alignment of MADS-box motifs. MADS-boxes conserved among members are shaded. Sequences were retrieved from NCBI: *S. cerevisiae* (Umc1; KZV08890.1), *M. oryzae* (MoMcm1; XP_003720973.1), and *U. maydis* (MCM1; AAB92597.1). A conserved 'hydrophobic patch' comprising predominantly hydrophobic amino acids is indicated (green line). In addition, the location of the putative DNA-binding α-helix is indicated (black line). Basic amino acids which play a critical role in DNA binding by SRF-like type transcription factors are highlighted (black *), as well as the two conserved lysine residues whose simultaneous mutation severely decreases DNA binding (red *). (B) MADS-box and EBV-NA3 domains predicted for PstMCM1-1 via NCBI. (C) MADS-Box domain predicted for PstMCM1-2 via NCBI.

Fig. S2. Transcript profiles of *PstMCM1-2* during *Pst* infection. Relative transcript levels of *PstMCM1-2* were calculated using the $2^{-\Delta\Delta CT}$ method with the endogenous reference gene *EF-1* and the values for ungerminated urediospores (US) set to 1. US, urediospores; 6–264 h, 6–264

hpi with CYR32 of wheat; PS, pycniospores on infected *B. shensiana*. Data represent the mean of three biological replicates ± SE (*, $P < 0.05$; **, $P < 0.01$).

Fig. S3. PstMCM1-1 localizes in the nucleus of wheat protoplasts. GFP signals and chloroplast auto-fluorescence are shown in columns one and two respectively. Overlay of both images is presented in the third column. Images of bright field from the same cell are shown in the fourth column. Bars, 10 μm.

Fig. S4. Sequence analysis on the PstbE1. (A) The HD motive in PstbE1 was predicted via NCBI. (B) Alignment of PstbE1 and PtbE1. The predicted HD motifs are indicated (red lines).

Fig. S5. Yeast-two-hybrid assays for a *PstMCM1-1* interaction with PstSTE12 and PstbE1. Screens were performed on SD-L-W (left half of the figure) and SD-L-W-H-A with β-galactosidase (right half of the figure). The p53-T and Lam-T interactions were used as positive and negative controls respectively.

Fig. S6. Fragments of *PstMCM1-1* used for BSMV-HIGS and qRT-PCR assays. (A) Overview of the two fragments used for BSMV-HIGS, and the sequence stretch used for quantification via qRT-PCT. (B) Sequence alignment of *PstMCM1-1* and *PstMCM1-2* with the positions of the primers used for HIGS and qRT-PCR indicated.

Fig. S7. Transcript profiles of defense-related genes in BSMV:*PstMCM1-1* and BSMV:γ inoculated wheat plants. (A) Transcript abundance of pathogenesis-related proteins or defense-related genes in BSMV:*PstMCM1-1*-H inoculated wheat plants. (B) Transcript abundance of pathogenesis-related proteins or defense-related genes in BSMV:*PstMCM1-1*-B inoculated wheat plants. *TaPR1*, pathogenesis-related protein 1; *TaPR2*, β-1,3-glucanase; *TaAPX*, ascorbate peroxidase; *TaSOD*, superoxide dismutase; *TaCAT1*, catalase 1. The data were normalized to the *TaEF1* expression level. Values represent the means ± standard errors of three independent samples.

Table S1. Overview of orthologs used in the phylogenetic analysis.

Table S2. Primers used in this study.

Table S3. Ratio of curved germ tubes and percentage of appressorium formation.